Environment International 131 (2019) 104986

Contents lists available at ScienceDirect

Environment International

journal homepage: www.elsevier.com/locate/envint

Redistribution of intracellular and extracellular free & adsorbed antibiotic resistance genes through a wastewater treatment plant by an enhanced extracellular DNA extraction method with magnetic beads

Qing-Bin Yuan[a,b,*], Ya-Meng Huang[a], Wen-Bin Wu[a], Pengxiao Zuo[b], Nan Hu[a], Yong-Zhang Zhou[a], Pedro J.J. Alvarez[b,**]

[a] College of Environmental Science and Engineering, Nanjing Tech University, Nanjing 211816, China
[b] Department of Civil and Environmental Engineering, Rice University, Houston, TX 77251, USA

ARTICLE INFO

Handling Editor: Zhen Jason He

Keywords:
Magnetic beads
Wastewater treatment facility
Antibiotic resistance genes
Extracellular DNA
DNA extraction
Bacterial community

ABSTRACT

Due to the limitations of current extraction methods, extracellular DNA (eDNA) is rarely discerned from intracellular DNA (iDNA) despite having unique contributions to antibiotic resistance genes (ARGs) propagation. Furthermore, eDNA may be free (f-eDNA) or adsorbed to or suspended solids, including cells (a-eDNA), which affects ARG persistence and transmissivity. We developed a novel method using magnetic beads to separate iDNA, a-eDNA, and f-eDNA to assess how these physical states of ARGs change across a wastewater treatment plant. This method efficiently extracted eDNA (> 85.3%) with higher recovery than current methods such as alcohol precipitation, CTAB-based extraction, and DNA extraction kits (< 10%). Biological treatment and UV disinfection decreased the concentration of intracellular ARGs (iARGs) and adsorbed extracellular ARGs (a-eARGs), causing an increase of released free extracellular ARGs (f-eARGs). More ARGs were discharged through the wasted biosolids than in the effluent; iARGs and a-eARGs are prevalent in wasted biosolids ((73.9 ± 22.5) % and (23.4 ± 15.3) % of total ARGs respectively), while f-eARGs were prevalent in the effluent ((90.3 ± 16.5) %). Bacterial community analysis showed significant correlations between specific genera and ARGs (e.g., *Aeromonas*, *Pseudomonas* and *Acinetobacter* were strongly correlated with multidrug-resistance gene bla_{TEM}). This treatment system decreased the discharge of iARGs to receiving environments, however, increased eARG concentrations were present in the effluent, which may contribute to the environmental resistome.

1. Introduction

Despite their effectiveness at mitigating waterborne diseases, some wastewater treatment plants (WWTPs) act as breading grounds for antibiotic resistant bacteria (ARB) and spread associated antibiotic resistance genes (ARGs) to the environment through the discharge of secondary effluent and biosolids (Mao et al., 2014; Yu et al., 2017). However, little is known about the physical state of discharged ARGs, which could affect their persistence and transmissivity. For example, the fate of intracellular DNA (iDNA) is considerably different from extracellular DNA (eDNA) (Zhang et al., 2013), which can be further separated into free-eDNA (f-eDNA) and adsorbed-eDNA (a-eDNA) (i.e., bound to other particles including bacteria surfaces and colloids) (Bryzgunova et al., 2015; Laktionov et al., 2004).

The binding of eDNA to other particles, such as minerals or organic compounds provide protection against degradation by nucleases, increasing their persistence (Nagler et al., 2018; Nielsen et al., 2007). In contrast, f-eDNA may be degraded rapidly within several days (Barnes et al., 2014; Eichmiller et al., 2016a). Furthermore, bacterial uptake of f-eDNA may be easier than a-eDNA due to the size restriction of uptake channels (Kruger and Stingl, 2011).

Although the abundance is comparable to, or even higher than iDNA in some systems (Mao et al., 2014; Torti et al., 2018), eDNA is rarely separated from total DNA due to the limits of conventional DNA extraction methods (mainly filtration or centrifugation), which typically retain < 10% of eDNA (Eichmiller et al., 2016b; Li et al., 2018; Liang and Keeley, 2013; Zhang and Zhang, 2011). Current methods for extracting eDNA, such as alcohol precipitation, cetyltrimethylammonium bromide (CTAB)-based extraction, and DNA extraction kits, have been frequently used to analyze sediments, sludge, and biofilms (Corinaldesi

* Correspondence to: Q.-B. Yuan, College of Environment Science and Engineering, Nanjing Tech University, Nanjing 211816, Jiangsu, China.
** Corresponding author.
E-mail addresses: yuanqb@njtech.edu.cn (Q.-B. Yuan), alvarez@rice.edu (P.J.J. Alvarez).

https://doi.org/10.1016/j.envint.2019.104986
Received 8 April 2019; Received in revised form 31 May 2019; Accepted 30 June 2019

et al., 2005; Guo et al., 2018; Ogram et al., 1987; Renshaw et al., 2015; Torti et al., 2018; Wu and Xi, 2009; Zhang et al., 2018). However, these methods are complex and labor-intensive, and are mostly used for soil samples where eDNA is abundant and a-eDNA is the dominant form (Corinaldesi et al., 2005). They may not suitable for aquatic samples from environments where DNA concentrations are often low or f-eDNA is predominant (Nagler et al., 2018; Pote et al., 2009).

In this study, magnetic beads were used to extract eDNA from samples taken at multiple sites throughout a municipal wastewater treatment plant. Magnetic beads reversibly bind nucleic acids and are then separated by a magnetic field (Xiao et al., 2013). This technique has been used to extract bacterial genomes from serum and plasma (Berensmeier, 2006; Reverte et al., 2016). However, its application for environmental samples has not been reported, especially for extracting and separating different forms of eDNA that may influence ARG persistence and fate. Thus, different physical states of eDNA (i.e., a-eDNA and f-eDNA) were separated and quantified across a WWTP over one year. We demonstrate superior eDNA extraction efficiency than traditional methods, including alcohol precipitation, CTAB based method, and DNA isolation kit. We also quantified the occurrence of nine common ARGs in their various physical states across each unit in a WWTP and system discharge points to assess changes in the potential development and propagation of antibiotic resistance.

2. Materials and methods

2.1. Magnetic beads

Hydroxyl magnetic beads with a magnetite core (Fe_3O_4), an encapsulation, and a hydroxyl-coated surface were purchased from Wuxi Biomag Biotechnology Co., Ltd. (China). Prior to usage, the beads were suspended in 0.05% aqueous solution of sodium azide with a final stock concentration of 50 g/L. The physical and chemical properties of magnetic beads were characterized by Scanning Electron Microscope (SEM) and Fourier Transform Infrared Spectrometer (FTIR) (Fig. S1). As shown in Fig. S1, the beads had an average size of 10 μm and were well dispersed. The magnetic beads exhibit (C—O) absorption peaks at 1096 cm^{-1}, and (-OH) absorption peaks at 3225 cm^{-1}, which facilitates hydrogen bonding with nucleotides.

2.2. eDNA extraction

Activated sludge samples were passed through a 0.22-μm filter (Millipore, USA). Each of the four methods were used to extract eDNA from the activated sludge sample filtrate. Alcohol precipitation, CTAB based method and DNA isolation kit were conducted as detailed in Supplementary Info. Text 1–3 and associated references.

For the magnetic beads method, 10 mL isopropanol and 7.5 mL CL buffer (Proteinase K, 20 g/L in 30 mM Tris-Cl, Tiangen Biotech, China) were added to 5 mL sample filtrate and mixed thoroughly to remove impurities (e.g., proteins), then spiked with 20 μL of magnetic beads stock and vortexed for 3–4 min (Fig. 1A). The mixture was placed on a magnetic rack to precipitate the magnetic beads, and the supernatant without magnetic beads was discarded.

The magnetic beads were washed with 1 mL CW1 buffer (7 mol/L guanidine hydrochloride in 50% isopropanol), the magnetic rack was used again to remove the supernatant. The magnetic beads were then washed with 1 mL CW2 buffer (ethanol, 75%) twice and subsequently placed at room temperature for 5 min to evaporate the residual ethanol. Then, 30 μL of elution buffer (10 mM Tris-HCl, pH 8.5, preheated to 55 °C) was added to the magnetic beads followed by incubation for 5 min, and vortexed for 20 s every minute during incubation. Finally, the mixture was placed on the magnetic rack and the supernatant was collected for DNA analysis.

2.3. Optimizing the magnetic beads extraction method

The sample dosage and magnetic beads loading were optimized to improve the recovery efficiency of eDNA. To optimize the sample dosage, different volumes (1, 2, 5, 10 or 40 mL) were used for eDNA extraction. The volume of magnetic beads stock (50 g/L) added was 20 μL for all sample dosage tests. To determine the effect of magnetic beads dosage, 5, 10, 15 and 20 μL of magnetic beads stock (per mL sample) were used to extract eDNA, while the sample volume was kept at 2 mL.

Six pretreatment methods were assessed for separating a-eDNA from f-eDNA. Method I is the untreated control. For pretreatment method II, the sample was filtered through a 0.22-μm filter and the filter was washed twice with 5 mL Tris-EDTA (TE) buffer which then was mixed with sample filtrate prior to eDNA extraction. For method III, 20 mL of phosphate buffer (0.12 M NaH_2PO_4, 0.12 M Na_2HPO_4, pH = 4) was spiked into 100 mL sample, which was then filtered through a 0.22-μm filter. For method IV, the same 20 mL of phosphate buffer from method II was added but the mixture was shaken (150 rpm) for 20 min before filtering through a 0.22-μm filter. Method V involved adding 0.2 g polyvinylpyrrolidone (PVPP) and 20 mL phosphate buffer then vortexing for 20 min before filtering through a 0.22-μm filter. For method VI and VII, the sample was just vortexed for 10 min and 20 min respectively before filtering through a 0.22 μm filter.

Potential leakage of intracellular DNA was assessed by measuring the release of lactate dehydrogenase (LDH), as detailed in Supplementary Info. Text 4.

2.4. Sampling and DNA extraction

Samples were collected from a wastewater treatment plant located in Nanjing (China) with a capacity of 75,000 m^3 per day (80% municipal wastewater and 20% industrial wastewater). This biological treatment plant harbors two parallel activated sludge processes, Cyclic Activated Sludge Technology (CAST) and Modified Sequential Batch Reactor (MSBR) (Fig. 2). Biological Aerated Filter (BAF) is used to further remove organics and nitrogen. After UV disinfection, the effluent is directly discharged into the Yangtze River, the largest river in China. Details of the wastewater treatment process are given in Supplementary Materials Text 5 and Table S1. Seven samples were collected along with the WWTP process: four aqueous and three sludge samples (Fig. 2).

Samples were collected once per season over one year (May 2018, August 2018, December 2018 and March 2019). For each sampling site, three parallel 1-L samples were collected every 4 h over a 12-h period; and the composite 3-L sample was mixed in sterilized dark polyethylene plastic bottles and analyzed within 24 h of collection. The three forms of DNA were separately extracted from the above samples (Fig. 1B). First, the samples were passed through 0.22- μm filters. The filtration volumes of the samples are shown in Table S2. Filtrate ① was used to extract f-eDNA as described in Section 2.2. The membrane used to obtain filtrate ① was mixed with 10 mL phosphate buffer and vortexed at 25 °C for 20 min, and this solution was filtered through a new 0.22-μm filter. This yielded filtrate ②, which was used to extract a-eDNA using magnetic beads. The membranes were all put into DNA extraction tubes to extract iDNA using Fast DNA™ SPIN kit for soil (MP Biomedicals, USA). All extracted DNA was verified by agarose gel electrophoresis and quantified by Nanodrop 2000 (Thermo Fisher Scientific, USA).

2.5. Recovery assessment for eDNA by the magnetic beads method

Recovery efficiency of eDNA was assessed by using an external DNA standard (Mumy and Findlay, 2004). The standard free-DNA was a 16S rDNA fragment prepared as detailed in Supplementary Information Text 6, and was added into the filtrate of WWTP samples. A-eDNA is first pre-treated to become f-eDNA before DNA extraction by the

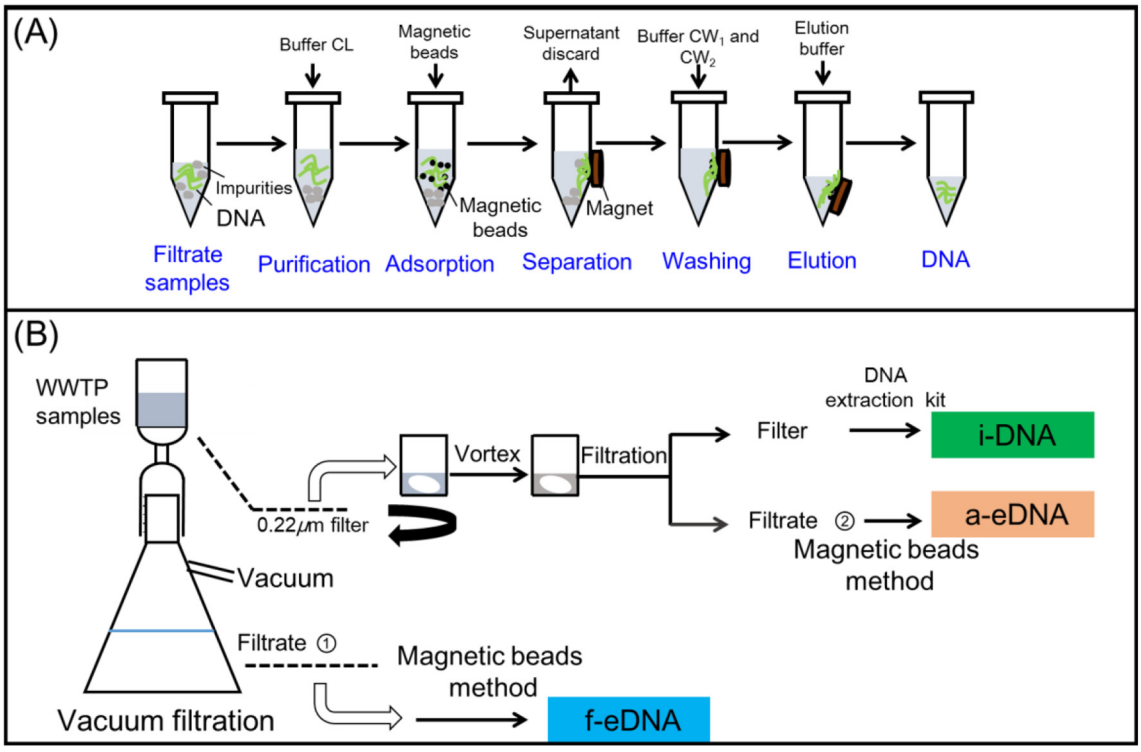

Fig. 1. (A). Illustration of magnetic beads method for eDNA extraction. (B). Isolation and extraction of iDNA, a-eDNA, and f-eDNA from WWTP samples.

magnetic beads method. As a result, free-DNA was used to assess the recovery efficiency of the magnetic beads method. The f-eDNA in the filtrate of collected samples (INF, CAST and EFF) was extracted by the magnetic beads method. The f-eDNA in the raw samples without standard free DNA addition was also extracted. The recovery efficiency was calculated according to the following formula (Eq. (1)).

$$\text{Recovery efficiency}\ (\%) = \frac{m_2 - m_1}{m_0} \times 100\% \quad (1)$$

where m_2 is the f-eDNA yield (ng) in samples with external DNA standard added, m_1 is the f-eDNA yield (ng) in samples without external DNA standard added, m_0 is the amount of external DNA standard added (ng).

2.6. Quantitative PCR

Quantitative polymerase chain reaction (qPCR) was performed as previously described (Wang et al., 2019), using a LightCycler 96 (Roche, Switzerland). Nine types of ARGs that are frequently present in WWTPs (Liu et al., 2018; Yuan et al., 2014; Zhang and Zhang, 2011) were investigated to quantify the abundance of the three physical states of DNA of interest. These ARGs were four tetracycline resistance genes (*tet*A, *tet*C, *tet*M and *tet*X), two sulfanilamide resistance genes (*sul*I and *sul*II), one class A β-lactamase (bla_{TEM}) and two macrolide resistance genes (*ere* A and *erm* B). Their primers have been validated by previous publications (Table S3). The PCR products of these nine ARGs were verified, purified, and cloned into *Escherichia coli*. The plasmids carrying each ARG were extracted as the standard ARG product. The

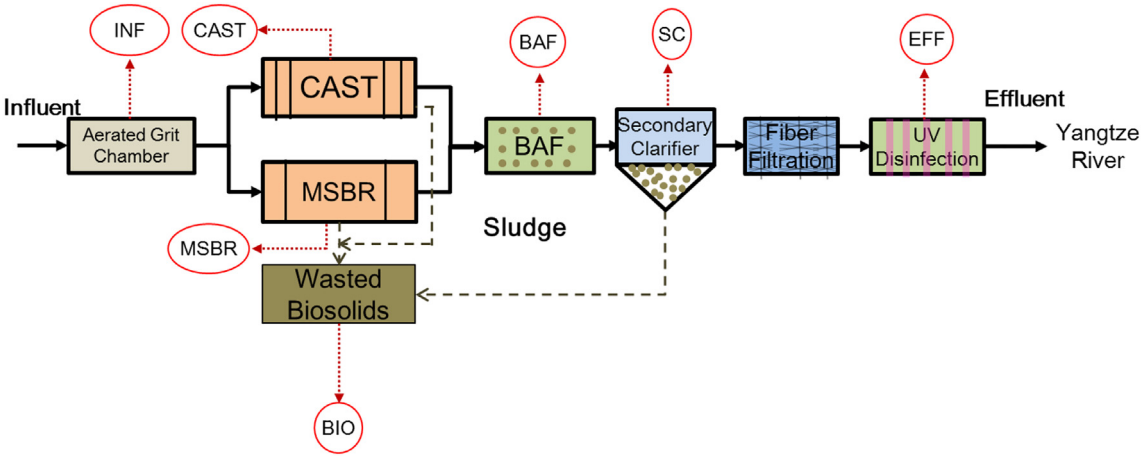

Fig. 2. Treatment processes and sampling sites. The seven red circles show sample collection locations, including four aqueous samples [influent (INF), biological aerated filter (BAF), effluent of secondary clarifier (SC), and final effluent after UV disinfection (EFF)] and three sludge samples [cyclic activated sludge tank (CAST), modified sequential batch reactor (MSBR), and wasted biosolids (BIO)]. (For interpretation of the references to colour in this figure legend, the reader is referred to the web version of this article.)

qPCRs were conducted in 8-strip tubes with a final volume of 20 μL, containing 10 μL 2 × SuperReal PreMix Plus (Tiangen Biotech, China), 2 μL 50 × Rox Reference Dye (Tiangen Biotech, China), 1 μL template DNA, 0.4 μL each primer, and 6.2 μL of double-distilled water.

The qPCR conditions included 95 °C for 15 min, followed by 40 cycles at 95 °C for 10s, annealing at defined temperatures (Table S3) for 20s and 64 °C for 30s. Each qPCR is performed in triplicate to ensure the deviation between triplicate samples were < 5%.The qPCR and operations of samples were same with the standard curves. The concentration of ARGs was calculated based on the number of cycles run for the sample. The amplification efficiencies of all qPCRs ranged from 88% to 110%. The abundance of 16S rDNA was also measured to assess the relative abundance of each ARG, which was defined as the ratio between an ARG abundance and 16S rDNA abundance.

2.7. Bacterial community analysis

The i-DNA and eDNA (including a-eDNA and f-eDNA) from influent (INF), activated sludge (CAST) and final effluent after UV disinfection (EFF) were used to examine the bacterial community and infer how its phylogenetic structure affected the observed ARG profile. The purified DNA samples were sent to the Shanghai Majorbio Bio-pharm Technology Co., Ltd. (China), with an Illumina miseq platform for bacterial 16S rDNA high-throughput amplification sequencing as described in a previous publication (Guo et al., 2015). DNA samples were amplified in triplicate by PCR using the primers 515F (5′-GTGCCAGC MGCCGCGG-3′) and 806R (5′-GGACTACHVGGGTWTCTAAT-3′). Sequence libraries of ~400 bp DNA fragments were prepared and sequenced according to the company's instructions. Analysis of the bacterial community composition, Shannon index, and heat map were all conducted on the free online platform of Majorbio I-Sanger Cloud Platform (www.i-sanger.com).

2.8. Data analysis

Mass balance analysis of ARGs was conducted by calculating the mass flow of ARGs at various sampling points as previously described (Fahrenfeld et al., 2014):

$$\text{Total mass flow of ARGs} = (C_i + C_f + C_a) \times Q \quad (2)$$

where C_i, C_f and C_a are the concentrations of iARG, f-eARG, and a-eARG, respectively, at a specific sampling point and Q is the average daily flow rate at the sampling point (Table S4).

The correlation between the relative abundance of ARGs in iDNA and eDNA and bacterial genera was explored by redundancy analysis (RDA). The correlation between the three types of ARGs was examined using canonical correlation analysis (CCA). Canoco 4.5 software (Wageningen University & Research, Netherlands) was utilized for the above analysis as described previously (Wang et al., 2019). The Monte Carlo permutation test was used to determine the significance; the number of replacements was 999. Finally, results were visualized using Canodraw 4.0 (Wageningen University & Research, Netherlands).

All statistical tests were conducted by two-tailed Student's *t*-test with statistical significance established at the 95% confidence level ($p < 0.05$) and null hypothesis as no significant difference existing between two data sets.

3. Results and discussion

3.1. Magnetic beads show significantly higher eDNA recovery than other methods

The magnetic beads extraction method yielded significantly better eDNA quality (A_{260}/A_{280} value of 1.7, indicating that interfering compounds were efficiently removed) and quantity (78 ng/mL) than alcohol precipitation, CTAB precipitation, and DNA extraction kits (Table 1). Magnetics beads were able to recover at least 20 times more eDNA than the other methods ($p < 0.05$) by using only 5 mL of sample. By comparison, the excessively low DNA concentration and improper sample volume required (200 to 300 mL for alcohol precipitation method and 1 mL for DNA extraction kit) demonstrated that current methods (alcohol precipitation, CTAB precipitation, and DNA extraction kits) were inefficient to extract eDNA from wastewater.

We postulate that DNA binds to magnetic beads through sodium cation bridges between the phosphate backbone of DNA and the hydroxyl group on the beads (Chang et al., 2015). These cation bridges have high affinity for eDNA because of its stronger negative charge than other constituents such as proteins and humic acid (Guo et al., 2016; Kozlowski, 2016). Furthermore, high recovery of DNA from magnetic beads can be achieved by eluting Na^+ with elution buffer (Adams et al., 2015). Finally, the high surface area of magnetic beads allows for more DNA binding sites (Holben et al., 1988) and higher recovery of eDNA per bead. Most eDNA could be extracted from water or sludge samples by the magnetic beads, making it ideal for eDNA extraction from small volume samples with low concentration of eDNA.

3.2. Enhanced eDNA recovery by optimizing magnetic beads method and pretreatment

Sample volume and magnetic beads dosage were optimized to improve the eDNA extraction efficiency (Fig. 3A and B). The recovered concentration increased as less volume of sample was processed, while the total yield of eDNA mass was greatest with 5 mL of sample. Apparently, smaller sample volumes increased the effective collision and binding between DNA and magnetic beads, but decreased the total eDNA present. In contrast, using a larger sample volume increased the extracted eDNA yield, but diluted the concentration of magnetic beads and lowered collision rates between the beads and eDNA, resulting in lower recovery. Compared to 2 mL, using 5 mL sample required disproportionally larger amounts of magnetic beads to extract the same amount of eDNA. To compromise between obtaining sufficient eDNA concentrations, eDNA yield and cost, 2 mL was chosen as the sample volume. Accordingly, eDNA yield and recovered concentration increased initially with magnetic beads dosage up to a maximum with 15 μL of magnetic beads per mL of sample (Fig. 3B), and decreased at higher dosages possibly due to beads aggregation hindering DNA extraction efficiency.

Three kinds of pretreatment methods were tested for separating a-eDNA and f-eDNA. These are: washing the membrane, decreasing the binding force, and vortex treatment (shown in Table 2). Comparing pretreatment methods II with the untreated control (Table 2), washing the membrane after filtration by TE buffer did not enhance eDNA concentration, indicating that little eDNA was filtered out or that washing did not remove eDNA from the filter. Adding phosphate buffer or PVPP did not improve the eDNA yield either (see results of pretreatment method III to V versus the untreated control, Table 2), possibly due to the samples not needing additional buffer to elute eDNA or that there was very little f-eDNA adsorbed to particles or membrane in the first place. Apparently these pretreatments did not exert sufficient force to separate f-eDNA and a-eDNA. Rather, eDNA quality (A_{260}/A_{280}) decreased by adding these solutions.

In contrast, vortexing (pretreatment methods VI and VII) significantly improved the eDNA yield and concentration ($p < 0.05$). When samples were vortexed for 10 min, the eDNA concentration increased slightly, but increased by 2.1-fold when they were vortexed for 20 min. Vortex pretreatment likely enhanced separation of a-eDNA from its associated particles, converting a-eDNA into f-eDNA. Cell membrane permeability assays were also conducted to ensure that vortex pretreatment was not damaging the cell membrane, since in preliminary experiments we found that some methods (e.g., sonication) would kill bacteria and cause the release of iDNA. No significant increase in LDH release was observed ($p > 0.05$) when the vortex period

Table 1
Volume for extraction, quality (A_{260}/A_{280}) and quantity (yield and concentration) of eDNA extracted by various methods.

Method	Extraction volume (mL)	A_{260}/A_{280}	Yield (ng)	Concentration (ng/mL)
Ethanol precipitation	200	2.1	330	2.8
Isopropanol precipitation	200	1.6	387	3.2
CTAB	30	2.5	3	0.2
DNA extraction kit	1	ND	ND	ND
Magnetic beads	5	1.7	234	78.0

Note: ND means non-detected.

was within 20 min (Fig. S2), indicating that the cell membrane integrity was retained. However, a significant increase in LDH release was observed when vortex period was increased to 60 min ($p < 0.05$), indicating damage of cell membrane and possibly leakage of iDNA.

By using 2 mL of vortexed (20 min) sample and 30 μL magnetic beads, the magnetic beads method could efficiently extract eDNA from wastewater, secondary effluent, and biosolids. The eDNA recovery efficiency was 85.3% from the influent, 93.0% from activated sludge, and 91.3% from the effluent when < 300 ng of eDNA standard was spiked (Fig. 3C). When the eDNA standard was increased to > 400 ng, the efficiency significantly decreased (data not shown), suggesting that the eDNA amount exceeded the adsorption capacity of the magnetic beads. However, these high concentration samples could be processed by diluting to a reasonable level (e.g., < 1000 ng/μL). By comparison, the recovery efficiency of current methods (alcohol precipitation, CTAB-based extraction, and DNA extraction kits) was all below 10%.

Generally, the concentrations of iARGs in our study were similar to total ARG concentrations reported in previous studies that utilized filtration for extraction (Chen and Zhang, 2013; Du et al., 2014). However, the total concentration of ARGs measured, including a-eDNA and f-eDNA, were generally higher than previous studies that only extracted iARGs (Di Cesare et al., 2016; Pruden et al., 2012; Zhang and Zhang, 2011), showing that eARGs were abundant in the WWTP and were a significant portion of total ARGs.

3.3. Changes in physical states of ARGs throughout the wastewater treatment process

The quality and quantity of i-DNA, a-eDNA and f-eDNA in the seven WWTP samples are presented in Table S5 and Fig. S3. Concentrations of iDNA, a-eDNA, and f-eDNA in influent were all on the order of 10^2 ng/mL. In activated sludge (CAST, MSBR and BIO), > 10^3 ng/mL of iDNA

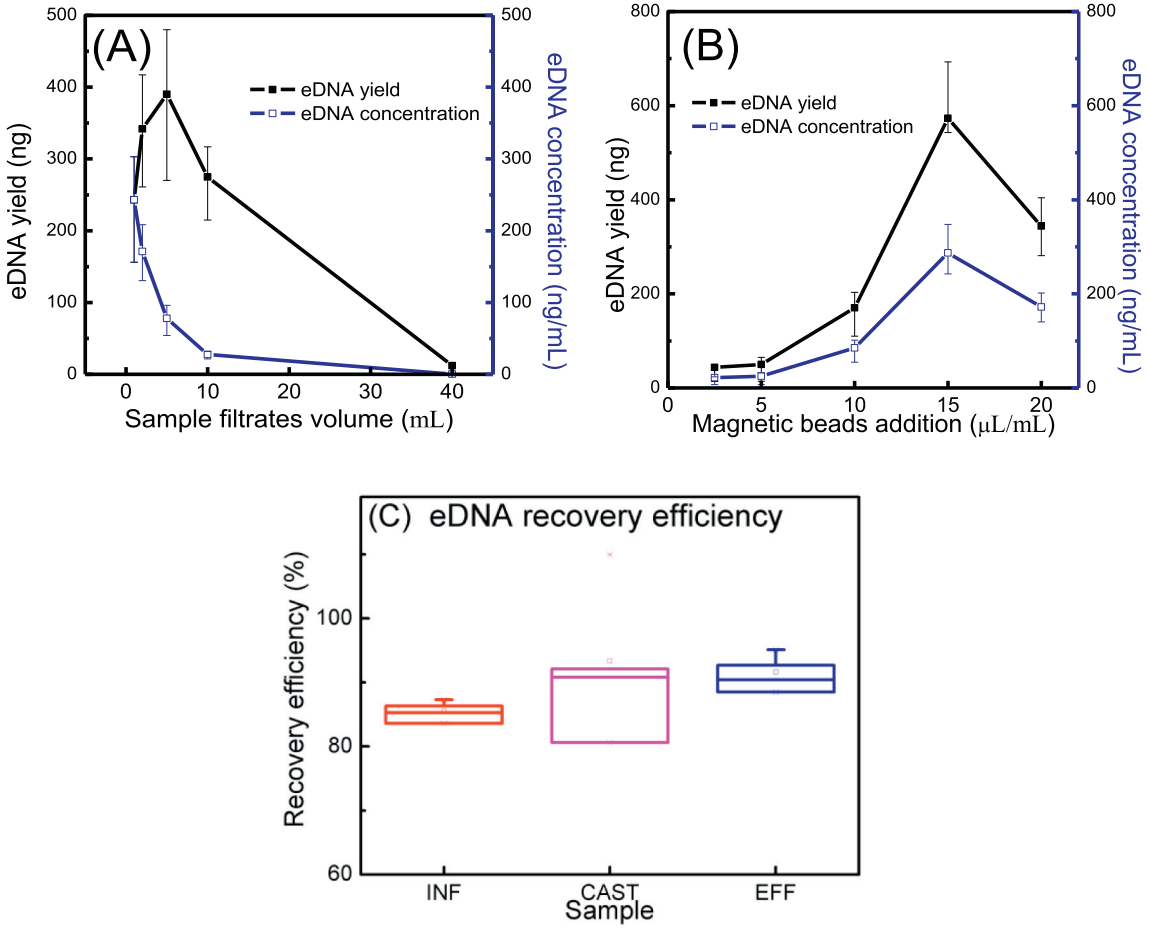

Fig. 3. (A) eDNA yield and concentration for different sample filtrates volume. The volume of magnetic beads was kept at 20 μL. (B) eDNA yield and concentration for different concentrations of magnetic beads added, the sample volume was kept at 2 mL. (C) The recovery efficiencies of eDNA from influent (INF), activated sludge (CAST) and effluent (EFF) by optimized magnetic beads method. This method extracted at least 85.3% of eDNA in samples from wastewater treatment plants.

Table 2
The quality (A_{260}/A_{280}) and quantity (yield and concentration) of eDNA after various pretreatment methods.

Pretreatment methods	A_{260}/A_{280}	Yield (ng)	Concentration (ng/mL)
I (blank control)	1.7	564	282.0
II (100 mL sample was filtered through a 0.22-μm filter, and the filter was washed twice by 5 mL of TE buffer)	2.4	285	142.5
III (20 mL phosphate buffer was spiked into 100 mL sample)	1.5	624	311.3
IV (100 mL sample was mixed with 20 mL phosphate buffer by shaking for 20 min)	1.6	710	354.8
V (100 mL sample was mixed with 20 mL phosphate buffer and 0.2 g PVPP)	1.2	525	262.5
VI (100 mL sample was vortexed for 10 min)	1.8	618	309.0
VII (100 mL sample was vortexed for 20 min)	1.6	1902	951.0

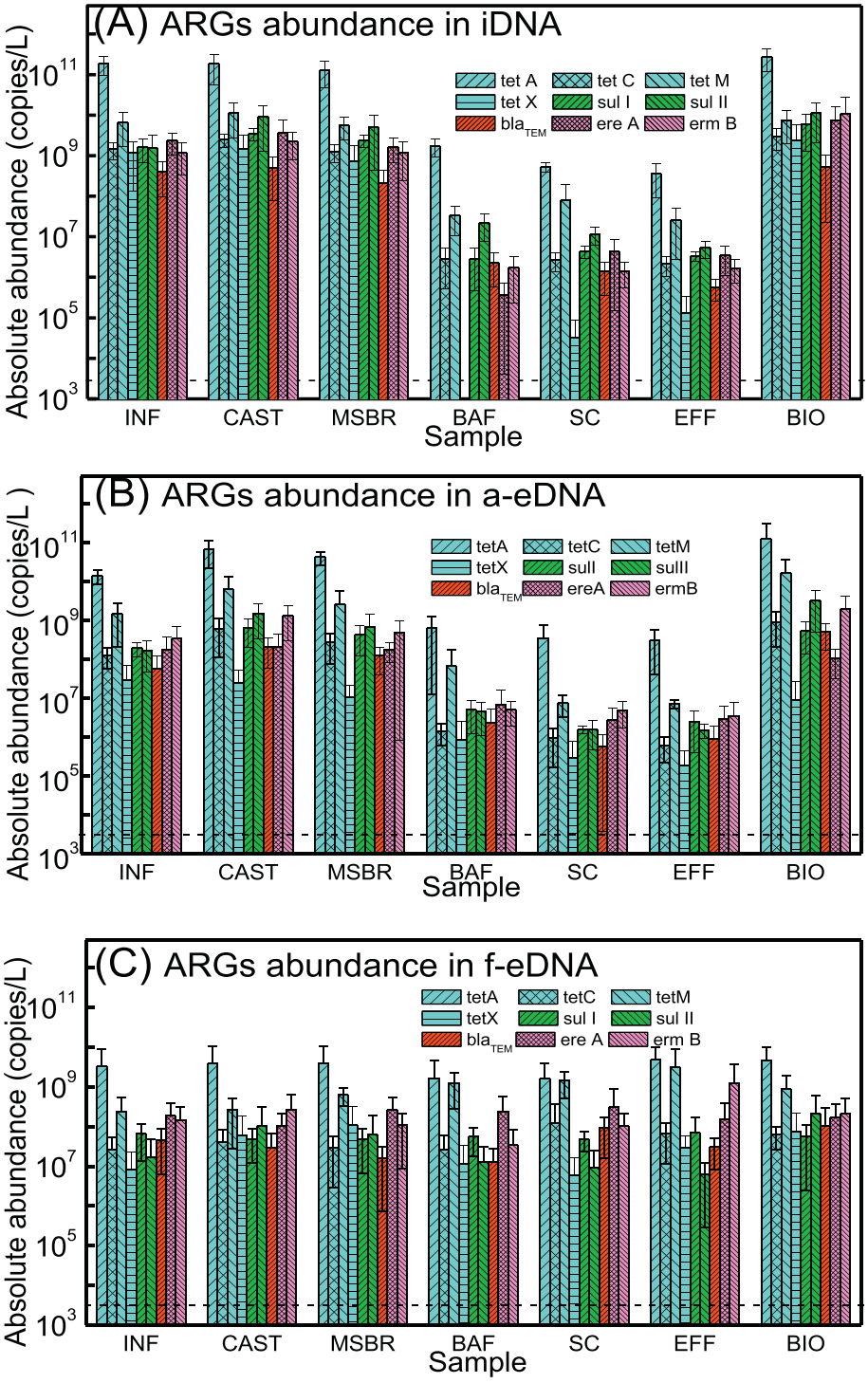

Fig. 4. Absolute abundance of nine ARGs in three forms of DNA during the wastewater treatment process. Abundance of iARGs and a-eARGs changed greatly with the wastewater treatment train, which increased in activated sludge and biosolids samples, but decreased in effluent samples. The change of f-eARGs was much smaller. The dash line represents the limit of detection (LOD). Nine ARGs include four tetracycline resistance genes (*tet*A, *tet*C, *tet*M and *tet*X), two sulfanilamide resistance genes (*sul*I and *sul*II), one class A β-lactamase (bla_{TEM}) and two macrolide resistance genes (*ere* A and *erm* B). INF, CAST, MSBR, BAF, SC, EFF and BIO represent seven sampling sites, including influent, cyclic activated sludge tank, modified sequential batch reactor, biological aerated filter, secondary clarifier, final effluent and biosolids.

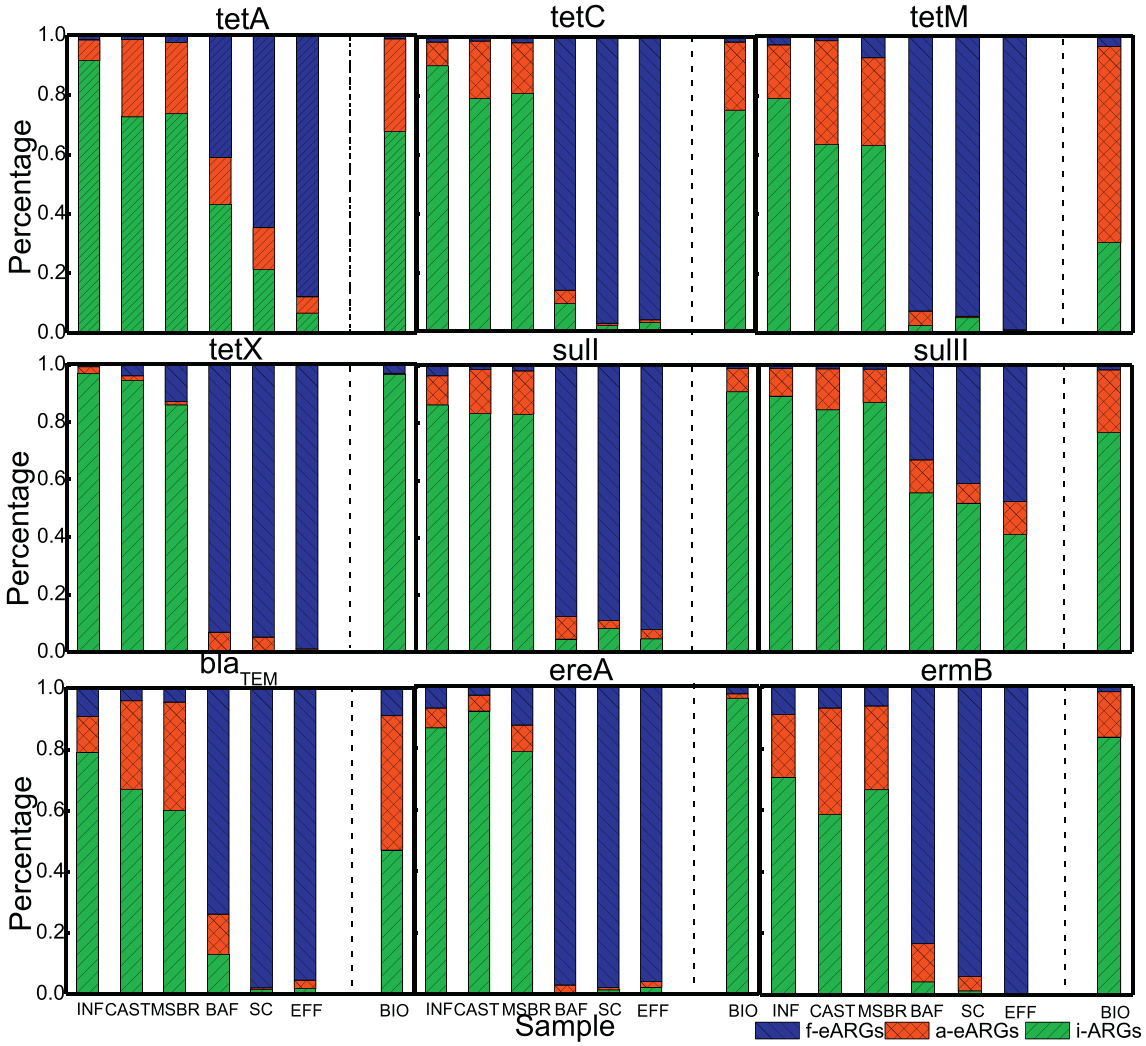

Fig. 5. Proportion of the three states ARGs (relative to total ARG concentration) from the seven sampling sites in WWTP. Generally, there was more iARGs in the influent, activated sludge and biosolids while there was more f-eARGs in the effluents. INF, CAST, MSBR, BAF, SC, EFF and BIO represent seven sampling sites, including influent, cyclic activated sludge tank, modified sequential batch reactor, biological aerated filter, secondary clarifier, final effluent and biosolids.

and a-eDNA were detected while f-eDNA was only on the order of 10^2 ng/mL. In the downstream water samples (BAF, SC and EFF), iDNA and a-eDNA concentration decreased to about 10^1 ng/mL level while f-eDNA remained on the order of 10^2 ng/mL.

In activated sludge, most ARGs in all three states became significantly more abundant than in the influent ($p < 0.05$) (Fig. 4). Compared to the influent, the relative proportion of ARGs as f-eARG in activated sludge did not change, but a-eARGs increased by (9.1 ± 7.7) % while iARGs decreased by (9.2 ± 6.3) % (Fig. 5). Nevertheless, iARGs were still the dominant form of ARGs in both influent and activated sludge (Fig. 5). Activated sludge promoted the proliferation of ARB and associated iARGs (Li et al., 2015; Wang et al., 2015), which became eARGs with the death of host ARB. However, iARGs are combined with proteins (Hammond et al., 2017), which are more likely to bind to particles (Silva et al., 2012); thus, iARGs predominately converted to a-eARGs. Furthermore, activated sludge is rich in particles that f-eARGs could combine with to form a-eDNA. Despite the increase in abundance, the relative abundance of most ARGs (normalized to 16s rDNA) decreased slightly ($p > 0.05$) in activated sludge (Fig. 6). This suggests insufficient selective pressure for ARGs, possibly due to the metabolic burden exerted by resistance plasmid maintenance and replication (Rysz et al., 2013).

Secondary clarification reduced the concentration of iARGs by 2.0–3.8 log and a-eARGs by 0.5–2.6 log, but did not reduce most f-eARGs because they were too small to be sufficiently precipitated (Fig. 7). UV disinfection further reduced the concentration of iARGs by 0.1–0.4 log (except *erm*B) and a-eARGs by 0.05–0.44 log, but increased f-ARGs by up to 1.2 log (Fig. 7). UV disinfection reduced iARGs by killing ARB, releasing a-eARGs combined with cell particles. Most a-eARGs would then become f-eARGs since there are very few particles in secondary effluent for f-eARGs to combine and reform a-eARGs. Continuous disassociation of a-eARGs into f-eARGs combined with higher degradation of ARB containing iARG than eARG by UV (McKinney and Pruden, 2012) resulted in insignificant reduction of f-eARGs during UV disinfection. UV disinfection did not greatly affect the relative abundance of ARGs to 16s rDNA of iARGs (Fig. 6), indicating that UV did not discriminate between ARGs and other DNA. Combined, clarification and UV disinfection reduced the concentration of iARGs by 2.4–4.1 log, a-eARGs by 0.7–2.7 log, and increased f-eARGs concentration by 0.03–1.1 log (Fig. 7).

Wastewater treatment process concentrated iARGs and c-ARGs into biosolids, accounting for (73.9 ± 22.5) % and (23.4 ± 15.3) % of total ARG concentration respectively. In contrast, f-eARGs was dominant in the effluent, accounting for (90.3 ± 16.5) % of total ARG concentration. The mass balance analysis (Fig. 8) indicates that more total mass flow of ARGs were discharged through biosolids (17%~65% of the influent ARGs) than the effluent (7%~50% of the influent ARGs). The total mass flow of ARGs discharged was 29% to 96% of that of the

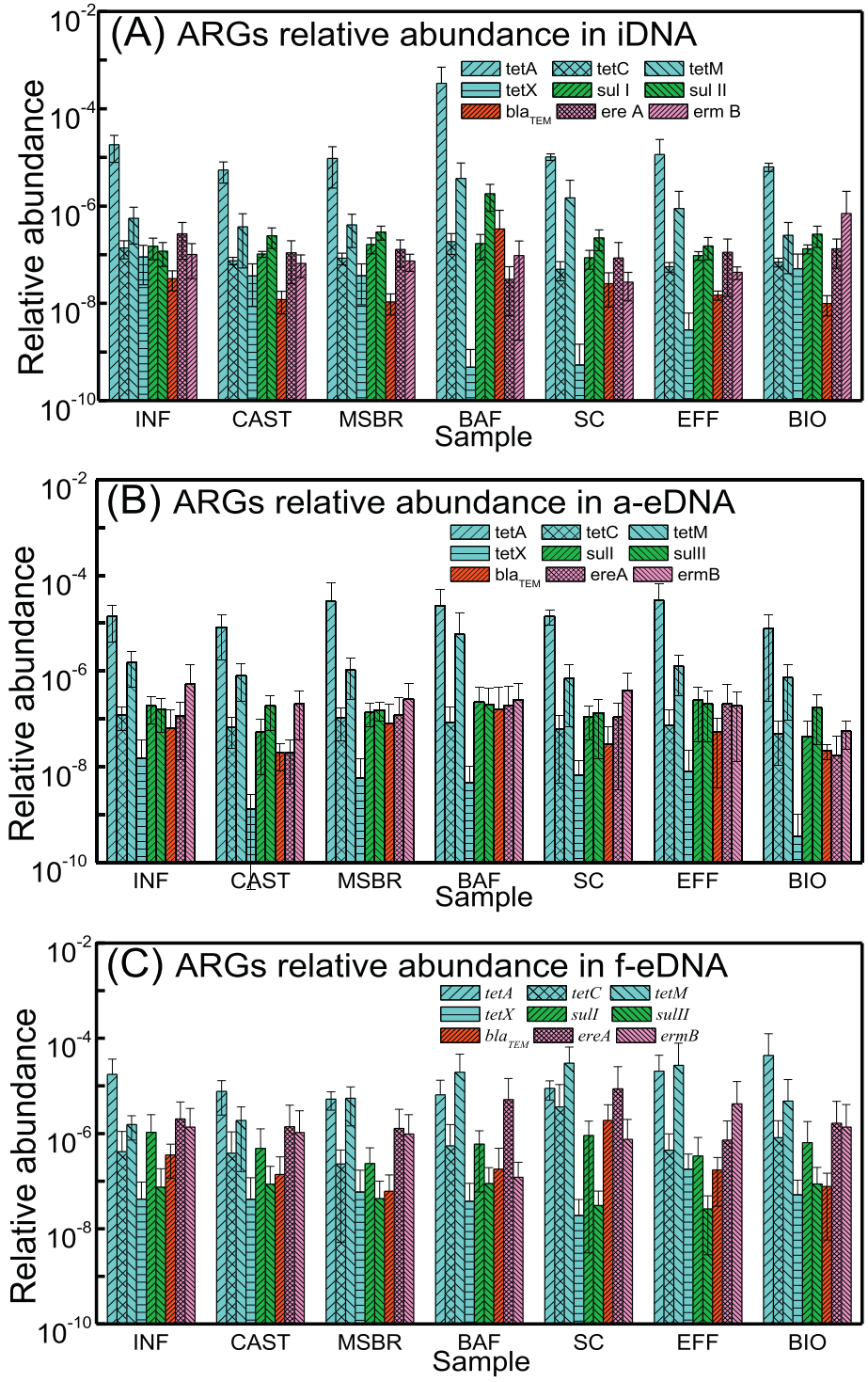

Fig. 6. Relative abundance of nine ARGs in three forms of DNA (normalized to 16S rDNA) across the wastewater treatment process. INF, CAST, MSBR, BAF, SC, EFF and BIO represent seven sampling sites, including influent, cyclic activated sludge tank, modified sequential batch reactor, biological aerated filter, secondary clarifier, final effluent and biosolids.

influent.

Free eDNA usually has lower persistence and transmissivity than a-eDNA or iDNA (Zhang et al., 2013), and this treatment system concentrated f-eARGs in the effluent while iARGs prevailed in the biosolids, which are applied as fertilizer after dewatering, which is conducive to survival of some ARB (Bala Subramanian et al., 2010). This raises the possibility of spreading antibiotic resistance in environments exposed to these biosolids (e.g., agricultural fields). Furthermore, the potential threats of the effluent cannot be overlooked which could contribute to the environmental resistome in receiving waters through transformation of indigenous bacteria (Luo et al., 2011).

3.4. Relative abundance of ARGs in iDNA and eDNA depends on abundance and diversity of bacterial hosts

The iDNA and eDNA of influent, effluent, and activated sludge

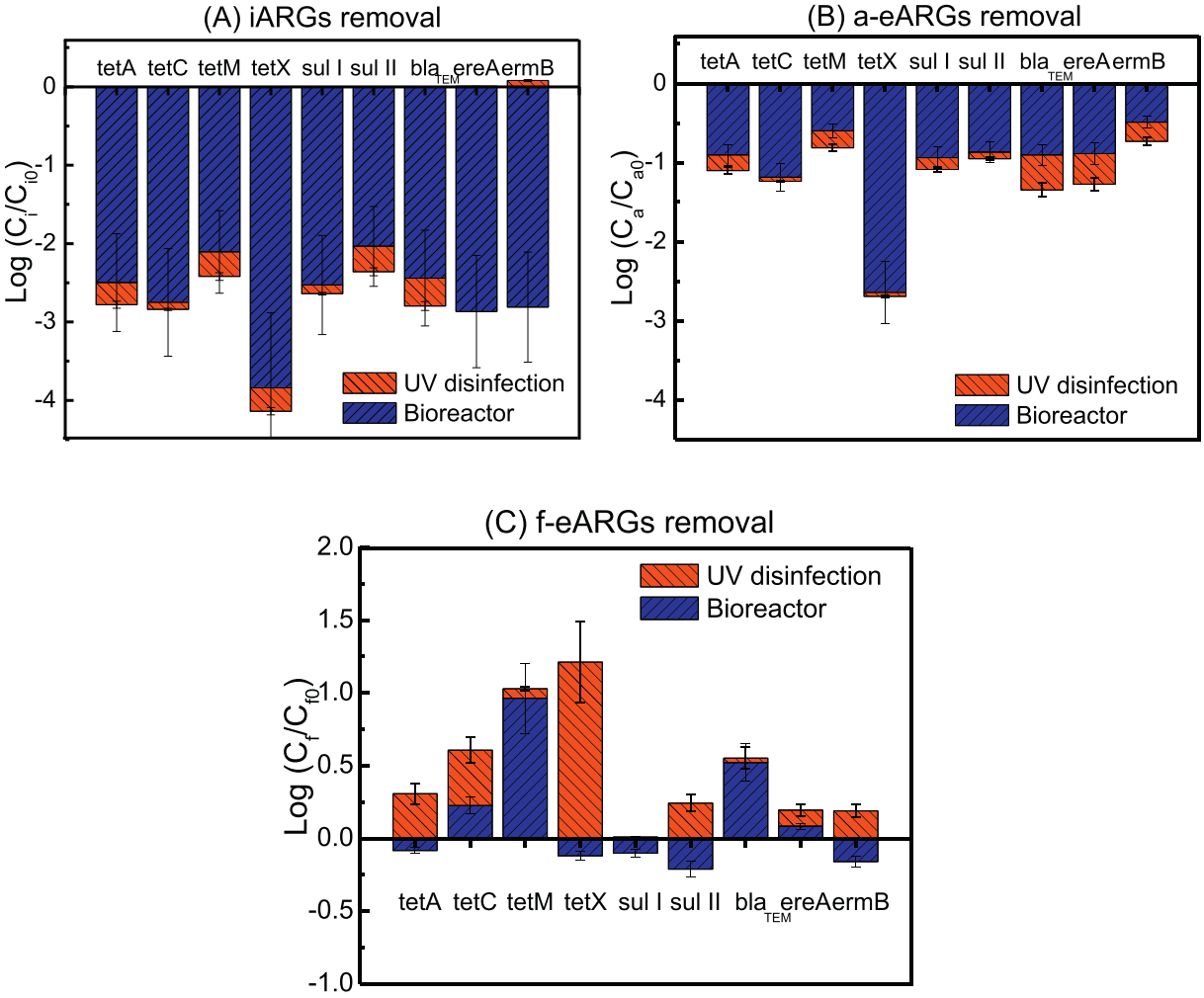

Fig. 7. Changes in the concentration of ARG in aqueous samples across a WWTP. Panels show log removal of iARGs (A), a-eARGs (B) and f-eARGs (C) by biological treatment processes and UV disinfection. The iARGs and a-eARGs were removed to a greater extent by biological process than f-eARGs. UV disinfection removed iARGs and a-eARGs, but caused the increase of most f-eARGs.

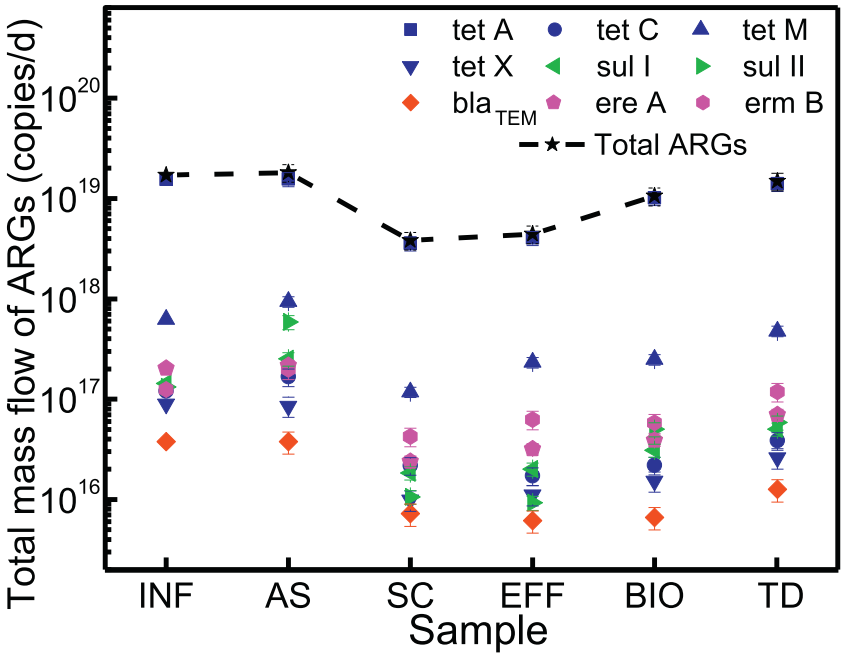

Fig. 8. Mass flow of ARGs across various treatment units (calculated using Eq. (2)). The total mass flow of ARGs slightly increased with bacterial growth in activated sludge (AS, sum of CAST and MSBR), and decreased in downstream aqueous samples (SC) as a result of biomass. More ARGs were discharged through biosolids than in the effluent. The rate of total ARGs discharge (TD, sum of EFF and BIO) was 29% to 96% of that of the influent rate.

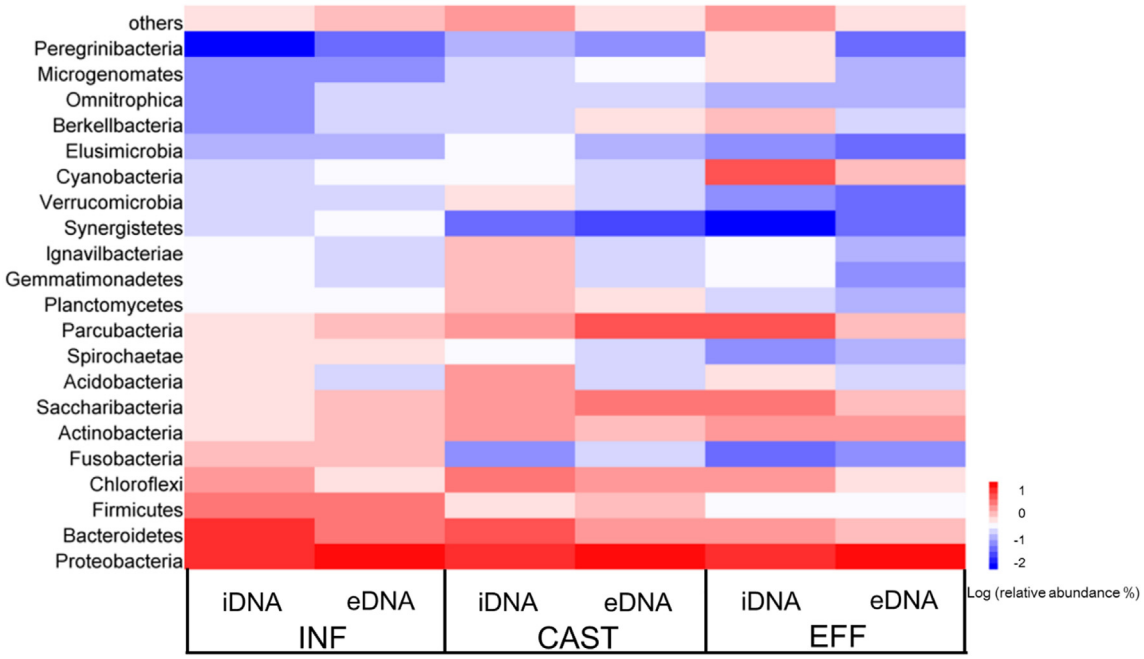

Fig. 9. Heat map of relative abundance of bacterial phyla in iDNA and eDNA of the influent (INF), activated sludge (CAST) and effluent (EFF). Log of relative abundance (%) were utilized for the heat map.

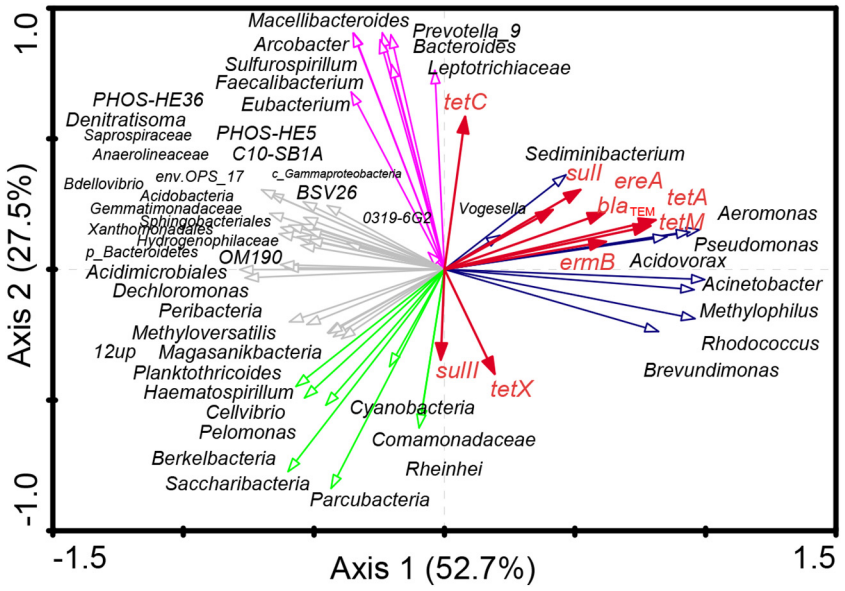

Fig. 10. Redundancy analysis shows the correlation between the relative abundance of ARGs and major genera, based on iDNA and eDNA sequences. ARGs are represented by solid arrows, while bacterial genera are represented by hollow arrows. Totally 51 genera are included here, which represent at least 1% of the total bacteria abundance in at least one sample. Nine genera represented by blue hollow arrows were positively correlated with *tet*A, *ere*A, *sul*I, *tet*M, bla_{TEM} and *erm*B; eight genera represented by pink hollow arrows were positively correlated with *tet*C; seven genera represented by green hollow arrows showed positive correlation with *tet*X and *sul*II. (For interpretation of the references to colour in this figure legend, the reader is referred to the web version of this article.)

samples was examined to gain insight on changes in bacteria phyla across the treatment process (Fig. 9 and Table S6) and discern potential ARG hosts (Fig. 10). Based on iDNA analysis, the most abundant phylum was Proteobacteria, followed by Bacteroidetes, Chloroflexi, and Saccharibacteria. The increase in relative abundance of common genera such as *Acinetobacter*, *Aeromonas*, *Brevundimonas*, *Acidovorax*, and *Rhodococcus* contributed to the abundance of Proteobacteria (Table S7). Interestingly, the abundance of eDNA from most phyla decreased except for Proteobacteria, suggesting a higher propensity for this phylum to release more DNA (i.e., conversion of its iDNA into eDNA). This observation agrees with the estimated Shannon index (*H*) (Table S8), indicating that the diversity of eDNA ($H = 3.6$) was significantly lower than that of iDNA ($H = 4.8$), possibly because of a relatively high abundance of eDNA originating from one phylum (e.g., Proteobacteria).

As expected, changes in the relative abundance of bacterial genera accounted for 98% of the variance of ARGs in iDNA and total eDNA (Fig. 10; 52.7% for Axis 1, 27.5% for Axis 2 and 17.8% for other Axis). This suggests that the relative abundance of an ARG present as iDNA versus eDNA depends on the fate of its bacterial host (e.g., live or dead), although some live cells may leak out plasmids (Nagler et al., 2018).

Among 51 genera, nine genera (*Vogesella*, *Sediminibacterium*, *Aeromonas*, *Pseudomonas*, *Acidovorax*, *Acinetobacter*, *Rhodococcus*, *Methylophilus* and *Brevundimonas*) showed positive correlations with *tet*A, *ere*A, *sul*I, *tet*M, bla_{TEM} and *erm*B; eight genera (*Prevotella_9*, *Bacteroides*, *Leptotrichiaceae*, *Macellibacterodies*, *Arcobacter*, *Sulfurospirillum*, *Faecalibacterium* and *Eubacterium*) exhibited positive correlations with *tetC*; seven genera (*Comamonadaceae*, *Rheinheimera*, *Parcubacteria*, *Cyanobacteria*, *Saccharibacteria*, *Berkelbacteria* and *Pelomonas*) exhibited positive correlations with *tet*X and *sul*II (Fig. 10). Several of these bacteria have been reported as hosts of the above ARGs

(Balassiano et al., 2007; Ferreira et al., 2016; Kielak et al., 2016; Ryan and Pembroke, 2018; Shi et al., 2018). Furthermore, *Aeromonas*, *Pseudomonas*, and *Acinetobacter* species have been reported to harbor bla_{TEM} (Banerjee et al., 2017; Chen et al., 2011; Jovcic et al., 2011), which endows resistance against beta-lactam antibiotics (i.e., a "superbug" gene). There were another 27 genera that showed no or even negative correlation with ARGs. Further studies are recommended to determine whether species with positive correlation to ARGs are major hosts of ARGs or if they replicate and release ARGs to a greater extent than those genera that showed no or negative correlations. If so, development of specific strategies to control these genera (including bacteriophage-based specific control (Yu et al., 2017)), should be considered to mitigate their contribution to ARG propagation.

4. Conclusions

Magnetic beads significantly enhance the extraction of eDNA, offering a practical method to study the fate of ARGs through wastewater treatment plants and assess how different processes affect the physical states of ARGs. When assessing risks of ARG transfer, determining the physical state of ARGs can now be a logical first step facilitated by our novel method. A redistribution of ARGs among iDNA, a-eDNA, and f-eDNA occurred through the wastewater treatment train. The iARGs were dominant in the influent and their abundance increased in bioreactors, consistent with bacteria growth. Subsequent bacterial decay (e.g., during disinfection) resulted in ARB releasing iARGs, which becomes a-eARGs or f-eARGs. Bacterial community analysis showed some significant correlations between specific genera and ARGs.

The wastewater treatment process significantly decreased the abundance of iARGs and a-eARGs; however, it increased the abundance of f-eARGs. ARGs in the effluent were predominantly in the form f-eDNA, whereas they were mainly iDNA in wasted biosolids. More ARGs were discharged through biosolids than through the effluent. The prevalence of f-eARGs in the effluent (which could transform indigenous bacteria) and inside whole cells in wasted biosolids (which could propagate resistance through conjugation) indicate that some WWTPs do not contribute equally to the antibiotic resistome in different receiving environments. This underscores the need for technological innovation to improve fundamental understanding of ARG fate and persistence. Knowledge of the physical state of ARG offers an enhanced perspective on their propagation potential, which could not be readily examined before and perhaps incorrectly attributed to other factors.

Declaration of Competing Interest

The authors declare that they have no known competing financial interests or personal relationships that could have appeared to influence the work reported in this paper.

Acknowledgements

Qing-Bin Yuan and Ya-Meng Huang contributed equally to the paper. We thank the workers in the wastewater treatment plant for their logistic support during sampling. This work was supported by the National Natural Science Foundation of China [grant number 51608260] and State Key Laboratory of Pollution Control and Resource Reuse Foundation [grant number PCRRF16029]. Pengxiao Zuo and Pedro Alvarez were supported by the NSF PIRE HEARD [grant number OISE-1545756].

Appendix A. Supplementary data

Supplementary data to this article can be found online at https://doi.org/10.1016/j.envint.2019.104986.

References

Adams, N.M., Bordelon, H., Wang, K.K., Albert, L.E., Wright, D.W., Haselton, F.R., 2015. Comparison of three magnetic bead surface functionalities for RNA extraction and detection. ACS Appl. Mater. Interfaces 7 (11), 6062–6069.
Bala Subramanian, S., Yan, S., Tyagi, R.D., Surampalli, R.Y., 2010. Extracellular polymeric substances (EPS) producing bacterial strains of municipal wastewater sludge: isolation, molecular identification, EPS characterization and performance for sludge settling and dewatering. Water Res. 44 (7), 2253–2266.
Balassiano, I.T., Bastos Mdo, C., Madureira, D.J., Silva, I.G., Freitas-Almeida, A.C., Oliveira, S.S., 2007. The involvement of tetA and tetE tetracycline resistance genes in plasmid and chromosomal resistance of Aeromonas in Brazilian strains. Mem. Inst. Oswaldo Cruz 102 (7), 861–866.
Banerjee, T., Pal, S., Das, A., 2017. Emergence of Aeromonas spp. Harboring Multiple Carbapenemase-encoding Genes from Hospital Sewage. J Lab Physicians 9 (1), 64–65.
Barnes, M.A., Turner, C.R., Jerde, C.L., Renshaw, M.A., Chadderton, W.L., Lodge, D.M., 2014. Environmental conditions influence eDNA persistence in aquatic systems. Environ Sci Technol 48 (3), 1819–1827.
Berensmeier, S., 2006. Magnetic particles for the separation and purification of nucleic acids. Appl. Microbiol. Biotechnol. 73 (3), 495–504.
Bryzgunova, O.E., Tamkovich, S.N., Cherepanova, A.V., Yarmoshchuk, S.V., Permyakova, V.I., Anykeeva, O.Y., Laktionov, P.P., 2015. Redistribution of free- and cell-surface-bound DNA in blood of benign and malignant prostate tumor patients. Acta Nat. 7 (2), 115–118.
Chang, Y.Y., Xie, S.B., Chai, Y.Q., Yuan, Y.L., Yuan, R., 2015. 3,4,9,10-Perylenetetracarboxylic acid/o-phenylenediamine nanomaterials as novel redox probes for electrochemical aptasensor systems based on an Fe3O4 magnetic bead as a nonenzymatic catalyst. Chem. Commun. 51 (36), 7657–7660.
Chen, Y., Zhou, Z.H., Jiang, Y., 2011. Emergence of NDM-1-producing Acinetobacter baumannii in China. Journal of Antimicrobial Chemotherapy 66 (6), 1255–1259.
Chen, H., Zhang, M., 2013. Occurrence and removal of antibiotic resistance genes in municipal wastewater and rural domestic sewage treatment systems in eastern China. Environ. Int. 55, 9–14.
Corinaldesi, C., Danovaro, R., Dell'Anno, A., 2005. Simultaneous recovery of extracellular and intracellular DNA suitable for molecular studies from marine sediments. Appl. Environ. Microbiol. 71 (1), 46–50.
Di Cesare, A., Eckert, E.M., D'Urso, S., Bertoni, R., Gillan, D.C., Wattiez, R., Corno, G., 2016. Co-occurrence of integrase 1, antibiotic and heavy metal resistance genes in municipal wastewater treatment plants. Water Res. 94, 208–214.
Du, J., Geng, J., Ren, H., Ding, L., Xu, K., Zhang, Y., 2014. Variation of antibiotic resistance genes in municipal wastewater treatment plant with A2O-MBR system. Environ. Sci. Pollut. Res. 22 (5), 3715–3726.
Eichmiller, J.J., Best, S.E., Sorensen, P.W., 2016a. Effects of temperature and trophic state on degradation of environmental DNA in lake water. Environ Sci Technol 50 (4), 1859–1867.
Eichmiller, J.J., Miller, L.M., Sorensen, P.W., 2016b. Optimizing techniques to capture and extract environmental DNA for detection and quantification of fish. Mol. Ecol. Resour. 16 (1), 56–68.
Fahrenfeld, N., Knowlton, K., Krometis, L.A., Hession, W.C., Xia, K., Lipscomb, E., Libuit, K., Green, B.L., Pruden, A., 2014. Effect of manure application on abundance of antibiotic resistance genes and their attenuation rates in soil: field-scale mass balance approach. Environ Sci Technol 48 (5), 2643–2650.
Ferreira, S., Queiroz, J.A., Oleastro, M., Domingues, F.C., 2016. Insights in the pathogenesis and resistance of Arcobacter: a review. Crit. Rev. Microbiol. 42 (3), 364–383.
Guo, M.T., Yuan, Q.B., Yang, J., 2015. Insights into the amplification of bacterial resistance to erythromycin in activated sludge. Chemosphere 136, 79–85.
Guo, Z., Wang, Y., Yang, A., Yang, G., 2016. The effect of pH on charge inversion and condensation of DNA. Soft Matter 12 (31), 6669–6674.
Guo, X., Yang, Y., Lu, D., Niu, Z., Feng, J., Chen, Y., Tou, F., Garner, E., Xu, J., Liu, M., Hochella, M.F., 2018. Biofilms as a sink for antibiotic resistance genes (ARGs) in the Yangtze Estuary. Water Res. 129, 277–286.
Hammond, C.M., Stromme, C.B., Huang, H., Patel, D.J., Groth, A., 2017. Histone chaperone networks shaping chromatin function. Nat Rev Mol Cell Biol 18 (3), 141–158.
Holben, W.E., Jansson, J.K., Chelm, B.K., Tiedje, J.M., 1988. DNA probe method for the detection of specific microorganisms in the soil bacterial community. Appl. Environ. Microbiol. 54 (3), 703–711.
Jovcic, B., Lepsanovic, Z., Suljagic, V., Rackov, G., Begovic, J., Topisirovic, L., Kojic, M., 2011. Emergence of NDM-1 metallo-beta-lactamase in Pseudomonas aeruginosa clinical isolates from Serbia. Antimicrob Agents Chemother 55 (8), 3929–3931.
Kielak, A.M., Barreto, C.C., Kowalchuk, G.A., van Veen, J.A., Kuramae, E.E., 2016. The ecology of Acidobacteria: moving beyond genes and genomes. Front. Microbiol. 7, 744.
Kozlowski, L.P., 2016. IPC - isoelectric point calculator. Biol. Direct 11 (1), 55.
Kruger, N.J., Stingl, K., 2011. Two steps away from novelty - principles of bacterial DNA uptake. Mol. Microbiol. 80 (4), 860–867.
Laktionov, P.P., Tamkovich, S.N., Rykova, E.Y., Bryzgunova, O.E., Starikov, A.V., Kuznetsova, N.P., Vlassov, V.V., 2004. Cell-surface-bound nucleic acids: free and cell-surface-bound nucleic acids in blood of healthy donors and breast Cancer patients. Ann. N. Y. Acad. Sci. 1022, 221–227.
Li, A.D., Li, L.G., Zhang, T., 2015. Exploring antibiotic resistance genes and metal resistance genes in plasmid metagenomes from wastewater treatment plants. Front. Microbiol. 6, 1025.
Li, F., Peng, Y., Fang, W., Altermatt, F., Xie, Y., Yang, J., Zhang, X., 2018. Application of environmental DNA metabarcoding for predicting anthropogenic pollution in rivers.

Environ Sci Technol 52 (20), 11708–11719.
Liang, Z., Keeley, A., 2013. Filtration recovery of extracellular DNA from environmental water samples. Environ Sci Technol 47 (16), 9324–9331.
Liu, S.S., Qu, H.M., Yang, D., Hu, H., Liu, W.L., Qiu, Z.G., Hou, A.M., Guo, J., Li, J.W., Shen, Z.Q., Jin, M., 2018. Chlorine disinfection increases both intracellular and extracellular antibiotic resistance genes in a full-scale wastewater treatment plant. Water Res. 136, 131–136.
Luo, Y., Xu, L., Rysz, M., Wang, Y., Zhang, H., Alvarez, P.J., 2011. Occurrence and transport of tetracycline, sulfonamide, quinolone, and macrolide antibiotics in the Haihe River Basin, China. Environ Sci Technol 45 (5), 1827–1833.
Mao, D., Luo, Y., Mathieu, J., Wang, Q., Feng, L., Mu, Q., Feng, C., Alvarez, P.J., 2014. Persistence of extracellular DNA in river sediment facilitates antibiotic resistance gene propagation. Environ Sci Technol 48 (1), 71–78.
McKinney, C.W., Pruden, A., 2012. Ultraviolet disinfection of antibiotic resistant bacteria and their antibiotic resistance genes in water and wastewater. Environ Sci Technol 46 (24), 13393–13400.
Mumy, K.L., Findlay, R.H., 2004. Convenient determination of DNA extraction efficiency using an external DNA recovery standard and quantitative-competitive PCR. J. Microbiol. Methods 57 (2), 259–268.
Nagler, M., Insam, H., Pietramellara, G., Ascher-Jenull, J., 2018. Extracellular DNA in natural environments: features, relevance and applications. Appl. Microbiol. Biotechnol. 102 (15), 6343–6356.
Nielsen, K.M., Johnsen, P.J., Bensasson, D., Daffonchio, D., 2007. Release and persistence of extracellular DNA in the environment. Environ. Biosaf. Res. 6 (1–2), 37–53.
Ogram, A., Sayler, G.S., Barkay, T., 1987. The extraction and purification of microbial DNA from sediments. J. Microbiol. Methods 7 (2–3), 57–66.
Pote, J., Mavingui, P., Navarro, E., Rosselli, W., Wildi, W., Simonet, P., Vogel, T.M., 2009. Extracellular plant DNA in Geneva groundwater and traditional artesian drinking water fountains. Chemosphere 75 (4), 498–504.
Pruden, A., Arabi, M., Storteboom, H.N., 2012. Correlation between upstream human activities and riverine antibiotic resistance genes. Environ Sci Technol 46 (21), 11541–11549.
Renshaw, M.A., Olds, B.P., Jerde, C.L., McVeigh, M.M., Lodge, D.M., 2015. The room temperature preservation of filtered environmental DNA samples and assimilation into a phenol-chloroform-isoamyl alcohol DNA extraction. Mol. Ecol. Resour. 15 (1), 168–176.
Reverte, L., Prieto-Simon, B., Campas, M., 2016. New advances in electrochemical biosensors for the detection of toxins: nanomaterials, magnetic beads and microfluidics systems. A review. Anal. Chim. Acta 908, 8–21.
Ryan, M.P., Pembroke, J.T., 2018. Brevundimonas spp: emerging global opportunistic pathogens. Virulence 9 (1), 480–493.
Rysz, M., Mansfield, W.R., Fortner, J.D., Alvarez, P.J., 2013. Tetracycline resistance gene maintenance under varying bacterial growth rate, substrate and oxygen availability, and tetracycline concentration. Environ Sci Technol 47 (13), 6995–7001.
Shi, L., Liang, Q., Feng, J., Zhan, Z., Zhao, Y., Yang, W., Yang, H., Chen, Y., Huang, M., Tong, Y., Li, X., Yin, Z., Wang, J., Zhou, D., 2018. Coexistence of two novel resistance plasmids, blaKPC-2-carrying p14057A and tetA(A) -carrying p14057B, in Pseudomonas aeruginosa. Virulence 9 (1), 306–311.
Silva, A.F., Carvalho, G., Soares, R., Coelho, A.V., Barreto Crespo, M.T., 2012. Step-by-step strategy for protein enrichment and proteome characterisation of extracellular polymeric substances in wastewater treatment systems. Appl. Microbiol. Biotechnol. 95 (3), 767–776.
Torti, A., Jorgensen, B.B., Lever, M.A., 2018. Preservation of microbial DNA in marine sediments: insights from extracellular DNA pools. Environ. Microbiol. 20 (12), 4526–4542.
Wang, J., Mao, D., Mu, Q., Luo, Y., 2015. Fate and proliferation of typical antibiotic resistance genes in five full-scale pharmaceutical wastewater treatment plants. Sci. Total Environ. 526, 366–373.
Wang, R.N., Zhang, Y., Cao, Z.H., Wang, X.Y., Ma, B., Wu, W.B., Hu, N., Huo, Z.Y., Yuan, Q.B., 2019. Occurrence of super antibiotic resistance genes in the downstream of the Yangtze River in China: prevalence and antibiotic resistance profiles. Sci. Total Environ. 651 (Pt 2), 1946–1957.
Wu, J., Xi, C., 2009. Evaluation of different methods for extracting extracellular DNA from the biofilm matrix. Appl. Environ. Microbiol. 75 (16), 5390–5395.
Xiao, Y., Hui Wang, C., Li, X., Wang, B., 2013. Research on magnetic separation methods for the extraction of nucleic acids. Adv. Mater. 662, 343–347.
Yu, P.F., Mathieu, J., Lu, G.W., Gabiatti, N., Alvarez, P.J., 2017. Control of antibiotic-resistant bacteria in activated sludge using polyvalent phages in conjunction with a production host. Environ Sci Tech Let 4 (4), 137–142.
Yuan, Q.B., Guo, M.T., Yang, J., 2014. Monitoring and assessing the impact of wastewater treatment on release of both antibiotic-resistant bacteria and their typical genes in a Chinese municipal wastewater treatment plant. Environ Sci Process Impacts 16 (8), 1930–1937.
Zhang, T., Zhang, X.X., 2011. Occurrence, abundance, and diversity of tetracycline resistance genes in 15 sewage treatment plants across China and other global locations. Environ Sci Technol 45 (7), 2598–2604.
Zhang, Y., Snow, D.D., Parker, D., Zhou, Z., Li, X., 2013. Intracellular and extracellular antimicrobial resistance genes in the sludge of livestock waste management structures. Environ Sci Technol 47 (18), 10206–10213.
Zhang, Y., Li, A., Dai, T., Li, F., Xie, H., Chen, L., Wen, D., 2018. Cell-free DNA: a neglected source for antibiotic resistance genes spreading from WWTPs. Environ Sci Technol 52 (1), 248–257.